

On the Adiabaticity Contribution to the Rate of Outer-Sphere Electron Transfers. Reactions of Cytochrome *c* and Related Transition Metal Compounds

G. Ferraudi

Radiation Laboratory, Notre Dame, Indiana 46556-0579

Received October 5, 1999

Magnetokinetic effects were observed between 0 and 8 T in electron-transfer reactions of Ru(bipy)₃³⁺ with ferrous cytochrome *c*, Fe(bipy)₃²⁺, Fe(Me4-[14]1,3,8,10-tetraene-1,4,8,11-N₄)(solvent)₂²⁺, and Ru(NH₃)₆²⁺. The effects have been related to the adiabatic character of the reactions and rationalized in terms of a mechanism that incorporates the spin-orbit coupling, hyperfine-coupling, and Zeeman mechanism in the expression of the reaction rate constant.

Introduction

In the study of outer-sphere electron-transfer reactions, some experimentalists have assumed that the electronic transmission coefficient factor, κ_{el} , in the expression of the reaction rate constant,

$$k_{\text{et}} = \kappa_{\text{el}} \kappa_{\text{nu}} \nu_{\text{nu}} \quad (1)$$

κ_{nu} = nuclear transmission coefficient

ν_{nu} = nuclear frequency

is equal to 1.¹ This assumption leads to a rate constant, $k_{\text{et}} = \kappa_{\text{el}} \nu_{\text{nu}}$, which is only dependent on the Franck–Condon factors and their associated nuclear parameters. By contrast, other researchers have used $\kappa_{\text{el}} < 1$ in order to account for discrepancies between measured values of k_{et} and those calculated with $\kappa_{\text{el}} = 1$ and some assumed Franck–Condon model.

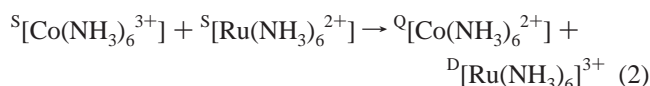
External perturbations that only affect k_{et} and leave κ_{nu} and ν_{nu} unchanged must lead to responses of k_{et} that can be used to probe the adiabatic character of electron-transfer reactions. The application of such external perturbations to this problem has been previously addressed in connection with reactions of ion pairs.^{1,2} Changes in the reaction rate constant by external magnetic fields result from perturbations that only change the electronic matrix element in a predictable manner and therefore provide information about κ_{el} . In this regard, the most elemental condition for the observation of magnetic field effects, MFE, on the reaction rate is $\kappa_{\text{el}} < 1$; i.e., the reaction is adiabatic relative to the zero-order potential surfaces or Ehrenfest sense.⁴

To the effects of this work, it is necessary to briefly describe several mechanisms that account for the observation of MFE in redox reactions.

(a) Radical Pair Mechanisms. The radical pair, RP, or the radical ion pair, RIP, mechanisms provide a solid theoretical

framework for the rationalization of such effects in some particular redox reactions involving radicals.^{3,5–8} In these mechanisms, radical pairs or radical ion pairs are stochastically joined in a given spin state. The rate of the dynamic evolution from the stochastically formed spin state to other available spin states is affected by the magnetic field. Since some of the quantum mechanical perturbations that determine such a dynamic evolution are common to the radical pair and electron-transfer mechanisms, they will be considered below in relation to the latter mechanism. Only those pairs that are formed or reach in time a state correlated with a state of the products are able to react. Pairs in states uncorrelated with the states of the products are separated before they react; i.e., their constituents are returned to the bulk. Literature examples have shown that these mechanisms successfully account for the observed magnetokinetic effect (MKE) in a variety of reactions between inorganic radicals and reactions between inorganic radicals and transition metal compounds.^{3c,d,5–7} Aside from these successes, these mechanisms do not explain the MKE in many outer-sphere electron-transfer reactions, at least in those reactions between transition metal compounds.

(b) Electron-Transfer Mechanisms. One example of such reactions where MKEs are not expected on the basis of the RP or RIP mechanisms is shown in eq 2.

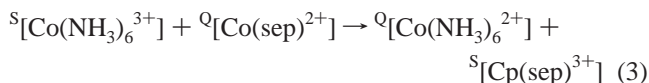


Superscripts on the left side of each species denote the spin state, e.g., S = singlet, D = doublet, Q = quartet. Complex

- (1) Jordan, R. *Reaction Mechanisms of Inorganic and Organometallic Systems*, 2nd ed.; Oxford, 1998; p 191.
- (2) Endicott, J. F.; Ramasami, T. *J. Phys. Chem.* **1986**, *90*, 3740.
- (3) (a) Ronco, S.; Ferraudi, G. *Inorg. Chem.* **1990**, *29*, 3961. (b) Ferraudi, G. *Mol. Phys.* **1997**, *91*, 273. (c) Ferraudi, G. *J. Phys. Chem.* **1993**, *97*, 11929. (d) Ferraudi, G. *J. Phys. Chem.* **1993**, *97*, 2793. (e) Ferraudi, G. *Pure Appl. Chem.* **1998**, *70*, 827.
- (4) Reynolds, W. L.; Lumry, R. W. *Mechanisms of Electron Transfer*, 1st ed.; The Ronald Press, 1966; pp 11, 12, 83.

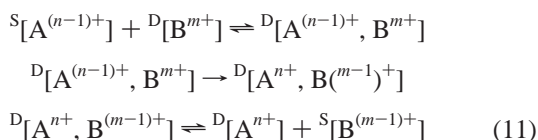
- (5) (a) Highes, M. E.; Corden, B. B. *J. Am. Chem. Soc.* **1989**, *111*, 4110. (b) Perito, R. P.; Corden, B. B. *Inorg. Chem.* **1988**, *27*, 1276.
- (6) (a) Taoka, S.; Padmakumar, R.; Grissom, C. B.; Banerjee, R. *Bioelectromagnetics* **1997**, *18*, 506. (b) Chagovetz, A. M. *J. Phys. Chem.* **1993**, *97*, 181. (c) Chagovetz, A. M. J.; Grissom, C. B. *J. Am. Chem. Soc.* **1993**, *115*, 12152.
- (7) (a) Klumpp, T.; Linsenmann, M.; Larson, S. L.; Limoges, B. R.; Burssner, D.; Krissinel, E. B.; Elliott, C. M.; Steiner, U. E. *J. Am. Chem. Soc.* **1999**, *121*, 1076. (b) Burssner, D.; Steiner, U. *Coord. Chem. Rev.* **1994**, *132*, 51. (c) Steiner, U. E.; Ulrich, T. *Chem. Rev.* **1989**, *89*, 51.
- (8) (a) Mori, Y.; Sakaguchi, Y.; Hayashi, H. *Chem. Phys. Lett.* **1999**, *301*, 365. (b) Wakasa, M.; Nishizawa, K.; Abe, H.; Kido, G.; Hayashi, H. *J. Am. Chem. Soc.* **1998**, *120*, 10565. (c) Mori, Y.; Sakaguchi, Y.; Hayashi, H. *Chem. Phys. Lett.* **1998**, *286*, 446.

and relatively intense MKEs have been observed in the rates of this and related reactions that involve reactants, d^6 metal ions, in singlet ground states.^{3b,c,e} Since the reactants' encounters can only produce singlet pairs in eq 2, the radical pair mechanism fails to account for the observed MKE. No excited states with higher spin multiplicities are accessible for mixing with the ground state of the reactants, and the intensity of the MKE is not substantially increased when one of the reactants is a paramagnetic species:



These magnetokinetic effects can be rationalized, however, by using quantum mechanical,^{9,10} or semiclassical models,¹¹ that include an electronic matrix element. MKE in outer-sphere electron-transfer reactions have been rationalized with a model based on the quantum mechanical perturbation theory.^{3b} A description of the mechanism is in the Appendix.

The electron-transfer mechanism can be tested by the observation of MKE in outer-sphere electron-transfer reactions of d^6 transition metal compounds with compounds of d^5 metal ions where reactants and products are all spin-paired species:



Since spin levels of the encounter pairs are the same as those of the products' pairs, the radical ion pair mechanism predicts no MKE in the rate of eq 11. By contrast to the radical ion pair mechanism, the quantum mechanical model foresees a dependence of the rate constant on B, similar to one previously observed with outer-sphere electron-transfer reactions of other transition metal compounds.³ The effect of the magnetic induction on the rate of several reactions involving spin-paired compounds of Fe(III/II) and Ru(III/II) couples were investigated in this work.

Experimental Section

Kinetic Measurements. To ensure the reproducibility of the MFE studied in this work, the laser intensity, the flow of the solution, and its temperature were controlled during the kinetic measurements. It was also necessary to measure optical density changes with relative errors equal to or smaller than 10^{-2} % for more than two reaction half-lifetimes, i.e., 200 ms. These conditions were fulfilled by introducing some modifications in a flash-photolysis setup previously used for the determination of time-resolved magnetic circular dichroism spectra of excited states.¹⁷ Solutions were flowed through a 1 cm cell placed in the cross bore cavity of a superconducting magnet, American Magnetics CH split coil, and were laser irradiated at a right angle with the probing

light. The steady-state probing light was coaxial with the magnetic induction, B . Magnetic inductions between 0 and 7 T, $1 \text{ T} \equiv 10^4 \text{ G}$, were generated with the superconducting magnet; they changed less than 0.2% from any given preselected value for periods longer than 10 h. Streams of thermostated N_2 were flowed through the magnet cavity and around the reaction cell whose temperature was monitored by a computer-interfaced sensor. Typical temperature fluctuations in the cavity were ± 0.1 °C. Solutions of the photolyte were deaerated with streams of ultrahigh purity Ar. The electronics and software used in previous work was modified in order to have an automated data collection that allowed an average of 2–2000 traces and simultaneously recorded the energy delivered by each flash and the temperature of the liquid in each determination. Traces recorded with laser powers or temperatures above or below preselected upper and lower limits were automatically rejected. The 10^3 traces averaged at each particular magnetic induction made it necessary to refresh the photolyte's solution after each determination but kept the solution static during the 200 ms of the measurement. An electronic flow control synchronized to the laser flash refreshed the solution in the cell after a 1 s delay of the laser trigger. Values reported for the ratio $k(B)/k(0)$, i.e., of the rate constants measured respectively under magnetic inductions $B \neq 0$ and $B = 0$, correspond to the most probable value of three to five determinations with each of them being an average of 1×10^3 to 2×10^3 traces. Each measurement of the rate constant at a given value B of the magnetic induction was always paired with another measurement

(12) A literature Hamiltonian,¹⁰ $\hat{H} = \hat{H}_A + \hat{H}_B + \hat{H}_C + \hat{H}_S + \hat{T}_e + \hat{T}_N + V_{BA} + V_{SA} + V_{eB} + V_{int}^S + V_{int}^C$ is composed of the following terms. \hat{H}_A and \hat{H}_B are electronic Hamiltonians for the cores. \hat{H}_C and \hat{H}_S are electronic Hamiltonians for the bulk solvent and the first coordination sphere. V_{BA} , V_{SA} , and V_{eB} are interaction potentials between cores and between a transferred electron and each core. \hat{T}_e is the kinetic energy operator of the transferred electron, and $\hat{T}_N = \hat{T}_{N,A} + \hat{T}_{N,B} + \hat{T}_{N,C} + \hat{T}_{N,S}$ is the sum of nuclear kinetic energy operators where A and B stand for the cores, C for the first coordination sphere, and S for the bulk solvent.^{9a} In the second-order perturbation treatment, the Fermi golden rule is derived by solving the equation of motion of the expansion coefficients,

$$\begin{aligned} i \frac{\partial C_{i,v}(t)}{\partial t} \sum_w C_{f,w}(t) H_{i,v:f,w} \cdot \exp\left(\frac{i}{\hbar} [E_{f,w}^0 - E_{i,v}^0] t\right) \\ - \frac{\partial C_{f,w}(t)}{\partial t} \sum_v C_{i,v}(t) H_{f,w:i,v} \cdot \exp\left(\frac{i}{\hbar} [E_{f,w}^0 - E_{i,v}^0] t\right) \end{aligned}$$

to find the expression for the probability $W_{i,v}$ for the evolution of a zero-order vibronic level $\langle i,v |$ to a vibronic manifold $\langle f,w |$. Such a probability in the form of a Fermi's second golden rule is

$$W_{i,v} = \frac{2\pi}{\hbar} \sum_w |H_{i,v:f,w}|^2 \delta(E_{f,w}^0 - E_{i,v}^0)$$

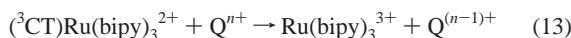
where $\delta(E_{f,w}^0 - E_{i,v}^0)$ is the Dirac delta that imposes the equality of the energies of the departure and arrival states as a condition for the evolution from one to another.

- (9) (a) Kestner, N. R.; Logan, J.; Jortner, J. *J. Phys. Chem.* **1974**, *78*, 2148. (b) Buhks, E.; Bixon, M.; Jortner, J.; Navon, G. *J. Phys. Chem.* **1981**, *85*, 3579. (c) Buhks, E.; Bixon, M.; Jortner, J.; Navon, G. *Inorg. Chem.* **1979**, *18*, 2014. (d) Jortner, J. *J. Chem. Phys.* **1976**, *64*, 4860. (e) VanDyne, R.; Fischer, S. *Chem. Phys.* **1974**, *5*, 183. (f) Hopfield, J. *Proc. Natl. Acad. Sci. U.S.A.* **1974**, *71*, 3640.
- (10) (a) Rips, I.; Jortner, J. *J. Chem. Phys.* **1987**, *87*, 2090. (b) Rips, I.; Jortner, J. *J. Chem. Phys.* **1987**, *87*, 6513. (c) Zusman, L. D. *Chem. Phys.* **1980**, *49*, 295. (d) Friedman, H. L.; Newton, M. D. *Discuss. Faraday Soc.* **1982**, *74*, 73. (e) Nadler, W.; Marcus, R. A. *J. Chem. Phys.* **1987**, *86*, 3906.
- (11) (a) Brunschwig, B. S.; Logan, J.; Newton, M. D.; Sutin, N. *J. Am. Chem. Soc.* **1980**, *102*, 5798. (b) Newton, M. D. *Int. J. Quantum Chem., Quantum. Chem. Symp.* **1980**, *14*, 383.

- (13) (a) Balhausen, C. J. *Molecular Electronic Structures of Transition Metal Complexes*; MacGraw-Hill: New York, 1979; Chapters 3 and 4. (b) Landaw, L. D.; Lifshitz, E. M. *Quantum Mechanics*; Pergamon: Oxford, 1974.
- (14) Margenaw, H.; Murphy, G. M. *The Mathematics of Physics and Chemistry*, 2nd ed.; D. Van Nostrand Co.: NJ, 1967.
- (15) The Hamiltonian can be divided in two parts, $\hat{H} = \hat{H}_{st} + \hat{H}(t)$, where \hat{H}_{st} is independent of time and includes only isotropic terms that survive the average in time over random motions. The time-dependent contribution, $\hat{H}(t)$, contains the anisotropic terms, identified by a subscript "an" in the text, and only survives over short periods, i.e., an autocorrelation time τ , thereby inducing relaxation among levels.
- (16) (a) Hayashi, H.; Nagakura, S. *Bull. Chem. Soc. Jpn.* **1984**, *57*, 322. (b) Sakaguchi, Y.; Hayashi, H.; Nagakura, S. *Bull. Chem. Soc. Jpn.* **1980**, *53*, 39. (c) Hayashi, H.; Nagakura, S. *Bull. Chem. Soc. Jpn.* **1978**, *51*, 2862. (d) Schulten, K.; Epstein, I. R. *J. Chem. Phys.* **1971**, *71*, 309. (e) Schulten, K.; Wolyness, P. G. *J. Chem. Phys.* **1978**, *68*, 3292. (f) McLauccchlan, K. A.; Scaly, R. C.; Wittman, J. M. *Mol. Phys.* **1978**, *36*, 1397. (g) Luders, K.; Salikkov, K. H. *Chem. Phys.* **1987**, *117*, 113. (h) Margulis, L. A.; Kudryakov, L. V.; Kuzmin, V. A. *Chem. Phys. Lett.* **1985**, *119*, 244. (i) Kaptein, R. *J. Am. Chem. Soc.* **1972**, *94*, 6251. (j) Kaptein, R. *J. Am. Chem. Soc.* **1972**, *94*, 6262. (k) Closs, G. L.; Trifunac, A. *J. Am. Chem. Soc.* **1970**, *92*, 2183.
- (17) Perkovic, M. W.; Ferraudi, G. *Inorg. Chim. Acta* **1997**, *254*, 1.

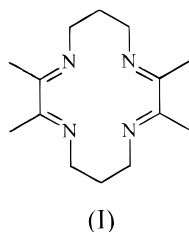
made on the same solution, under a zero magnetic induction, but with the same photochemical conditions otherwise.

The sequence of reactions, eqs 12–14 were used for the investigation of the MKE in the back-electron-transfer reaction, eq 14.



Quenching of the $\text{Ru}(\text{bipy})_3^{2+}$ charge-transfer excited state, $({}^3\text{CT})\text{Ru}(\text{bipy})_3^{2+}$, in eq 12 via electron transfer by Q^{n+} generates the oxidized $\text{Ru}(\text{III})$ and reduced $\text{Q}^{(n-1)+}$ products, eq 13. In studies of the reaction between $\text{Ru}(\text{bipy})_3^{3+}$ and $\text{Fe}(\text{bipy})_3^{2+}$, the $\text{Ru}(\text{III})$ was generated by quenching the excited state, eq 13, with $\text{Co}(\text{NH}_3)_6^{3+}$ in acid solutions. Rate constants of the back-electron-transfer reaction, eq 14, were calculated by a least-squares curve fitting to second-order or pseudo-first-order reaction kinetics. Solutions of the $\text{Ru}(\text{II})$ hexaammine complexes were prepared by adding the solid salts to liquids deaerated with streams of ultrahigh purity Ar and handled therein under an Ar atmosphere.

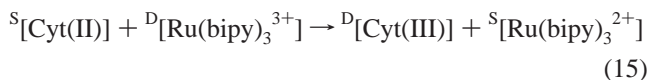
Materials. $[\text{M}(\text{bipy})_3](\text{ClO}_4)_2$ samples, $\text{M} = \text{Fe}$ or Ru , were obtained by three recrystallizations of $[\text{M}(\text{bipy})_3]\text{Cl}_2$, Alfa-Ventron, in aqueous solutions with NaClO_4 . Four recrystallizations of $[\text{Ru}(\text{NH}_3)_6]\text{Cl}_3$, Alfa-Ventron, were carried out by adding NaClO_4 to Ar-deaerated acidic solutions of the salt under an Ar atmosphere. The solid was kept and handled under an Ar atmosphere. Sigma Horse Heart Cytochrome *c*, Cyt(III), was used without further purification and its solutions handled according to a literature procedure.¹⁸ The macrocyclic complex, $[\text{Fe}(\text{Me}_4[14]-1,3,8,10\text{-tetraene-1,4,8,11-N}_4)(\text{OCH}_3\text{CH}_2\text{OH})](\text{ClO}_4)_2$ (**1**) was



prepared and purified by Rose's method.^{18d} Other materials were available from a previous study and used without purification.

Results

In the absence of an applied magnetic induction, the rate constant measured for the oxidation of ferrous cytochrome *c*, Cyt(II), by $\text{Ru}(\text{bipy})_3^{3+}$,



was in good agreement with results from a literature report.^{18a}

Under the influence of a magnetic induction, B , the rate constant showed a marked dependence on B between 0 and 8 T (Figure 3). A maximum amplitude of the MKE is attained at $B_{\text{max}} \approx 0.05$ T, i.e., a magnetic induction where the value of the rate is at a minimum. Above B_{max} , the rate constant approaches asymptotically the value recorded at 0 T with

(18) (a) Cho, K. C.; Che, C. M.; Cheng, F. C.; Choy, C. L. *J. Am. Chem. Soc.* **1984**, *106*, 6843. (b) Winkler, J. R.; Nocera, D. G.; Yocom, K. M.; Bordignon, N.; Gray, H. B. *J. Am. Chem. Soc.* **1984**, *106*, 5145. (c) Kostic, N. M.; Margalit, R.; Che, C. M.; Gray, H. B. *J. Am. Chem. Soc.* **1983**, *105*, 7765. (d) Reichgott, D. W.; Rose, N. J. *J. Am. Chem. Soc.* **1977**, *99*, 5152.

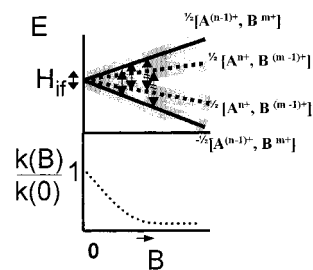


Figure 1. Simplified views of the effect of the magnetic induction, $B < 3$ T, upon the eq 11 relative rate constant, bottom, and the energy levels, top, of reactants $[\text{A}^{(n-1)+}, \text{B}^{m+}]$ and products $[\text{A}^{n+}, \text{B}^{(m-1)+}]$. The levels, represented by a nuclear configuration infinitesimally close to that of the activated complex, are degenerate and are separated by a magnetic induction $B = 0$. Unbroken vertical arrows show regions with connected levels enveloped within the width of the perturbation element H_{ij} connecting them and driving the spin evolution from one to another state. Only spin-flip transitions induced by dipolar interactions, \hat{I}_{SOC} , \hat{I}_{AFC} , are shown for the sake of simplicity. Broken arrows show regions where the magnetic induction has cut off the evolution among states. Contributions from a relaxation mechanism are not included.

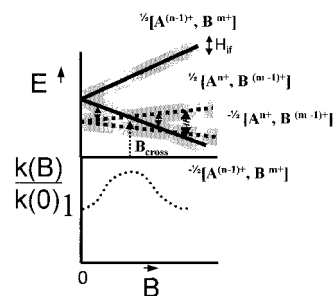


Figure 2. Simplified views of the effect of the magnetic induction, $B < 3$ T, upon the eq 11 relative rate constant, bottom, and the energy levels, top, of reactants $[\text{A}^{(n-1)+}, \text{B}^{m+}]$ and products $[\text{A}^{n+}, \text{B}^{(m-1)+}]$. The levels are represented by a nuclear configuration infinitesimally close to that of the activated complex and are separated by a gap $E \neq 0$ at $B = 0$. A spin-flip transition between levels crossing at $B = B_{\text{cross}}$ is effective at magnetic fields where gray areas overlap. Other aspects of the curves are as indicated for Figure 1.

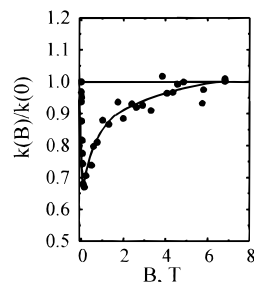


Figure 3. Effect of the magnetic induction B on the rate constant $k(B)$, normalized with respect to the rate constant $k(0)$ at $B = 0$, for the oxidation of Cyt(II) by $\text{Ru}(\text{bipy})_3^{3+}$, eq 14. The reaction is investigated in deaerated solutions buffered at pH 5.

increasing magnetic inductions. The observed magnetokinetic behavior of eq 15 and the reported discrepancy between calculated and measured rate constants provide support to the literature proposition that the electron-transfer reaction is nonadiabatic.^{18a,19}

The magnetokinetic effects were also investigated in a reaction of other low-spin $\text{Fe}(\text{II})$ complexes, eq 16, to verify that the curve in Figure 3 was not the result of some inadvertent conditions in the reaction; i.e., MKE dictated a symmetry-

(19) Chow, M.; Creutz, C.; Sutin, N. *J. Am. Chem. Soc.* **1977**, *99*, 1813.

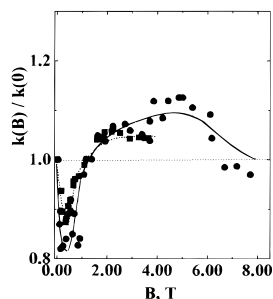


Figure 4. Effect of the magnetic induction B on the rate constant $k(B)$, normalized with respect to the rate constant $k(0)$ at $B = 0$, for the oxidation of $\text{Fe}(\text{bipy})_3^{2+}$ (○) or $\text{Fe}(\text{Me}_4\text{-[14]-1,3,8,10-tetraene-1,4,8,11-N}_4\text{)(solvent)}_2^{2+}$ (□) by $\text{Ru}(\text{bipy})_3^{3+}$, eq 15. Reactions are investigated in deaerated solutions buffered at pH 5.

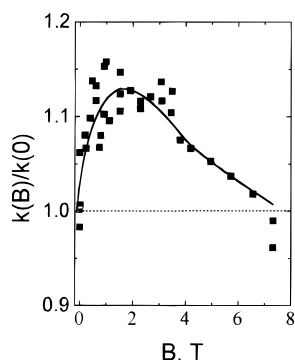
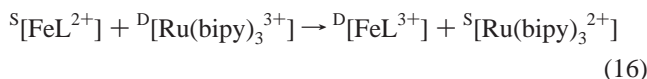


Figure 5. Effect of the magnetic induction B on the rate constant $k(B)$, normalized with respect to the rate constant $k(0)$ at $B = 0$, for the oxidation of $\text{Ru}(\text{NH}_3)_6^{3+}$ by $\text{Ru}(\text{bipy})_3^{3+}$, eq 16. The reaction is investigated in solutions deaerated with Ar and buffered at pH 5.

induced splitting and/or mixing of ground and excited states.

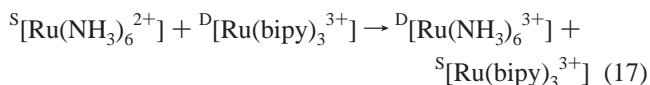


$\text{L} = (\text{bipy})_3,$

$(\text{Me}_4\text{-[14]-1,3,8,10-tetraene-1,4,8,11-N}_4\text{)(solvent)}_2$

In Figure 4, the dependences of the rate constants on the magnetic induction B also show an extreme in the amplitude of the MKE at $0.3 \leq B_{\text{max}} \leq 0.5$ T. A comparison of the MKE on the rate of eq 15 with those of eq 16 shows that values of the rate constants for the latter between 1 and 6 T are larger than the one at 0 T.

The magnetokinetic effects in outer-sphere electron transfers from a low-spin d^6 to a low-spin d^5 transition metal compound were also investigated in eq 17. By contrast with eq 16, this



reaction provides an electron exchange between similar metal ions and ensures that excited states and ground states of the reactants will not mix. By contrast to MKE shown in Figures 3 and 4, the rate constant, Figure 5, reaches no minimum value for $B < 1$ T and asymptotically approaches the value recorded at 0 T with increasing magnetic inductions, i.e., for $B > 1.5$ T.

Discussion

The pronounced magnetokinetic effects detected in the outer-sphere electron transfers, eq 15–17, lead to the following

conclusions. (a) Since the rates of nonadiabatic reactions are only changed by a magnetic induction,^{3,7c} these electron-transfer processes must be nonadiabatic. (b) The observed MKEs in the rates of eqs 2 and 15–17 are not accounted for by the radical pair mechanism. They must be rationalized on the basis of the B dependence of the electronic matrix element in eq 5. Reasons for the B -induced perturbations of those nonadiabatic channels are provided by the perturbational model described in the Introduction. Although the terms added after in $\hat{\lambda}_{\text{chg}}$, eq 5, have been defined elsewhere,^{3b,10,12} their main features and their application to an outer-sphere electron transfer of the type shown in eq 10 will be discussed in the following paragraphs.

The assumption that anisotropies in the \mathbf{g} tensor (Zeeman mechanism) and \mathbf{A} tensor (contact interaction) are averaged by fast random displacements of one reactant relative to the other was applied to $\hat{\lambda}$.¹⁵ This approximation has been previously used in reactions between inorganic radicals, radicals with coordination compounds, and outer-sphere electron transfers when $B < 2$ T.^{3,5–8} The rotation and internal vibrations, i.e., metal–ligand and ligand–skeletal, of one reactant referenced to the coordinates of the other can be used as time-dependent perturbations $V(t)$.^{3b} In times shorter than the autocorrelation time, the anisotropic components of \mathbf{g} and \mathbf{A} in the Hamiltonian and these $V(t)$ perturbations provide a “relaxation mechanism” for the conversion among spin states.^{3b} The contribution of the “relaxation mechanism” to MKE in eqs 15–17 will be discussed after those of the isotropic terms.

Isotropic Terms. 1. Hyperfine Coupling. An expansion of $\hat{\lambda}_{\text{hfc}}(B, A, t)$ by means of the shift operators, section a of Appendix, shows that it will couple off-diagonal states. For example, it has been shown elsewhere^{3b} that a reactants’ singlet electronic state, $|S\rangle|t_+\rangle$, with a +1 level of the nuclear triplet, $|t_+\rangle$, will evolve in time toward the -1 component of the products’ triplet electronic states, $|T_-\rangle|t_0\rangle$ and $|T_-\rangle|s\rangle$, with nuclear spin projections 0 and -1 .^{3b} In the case of the d^5/d^6 electron-transfer processes in eq 11, these terms allow the components of the reactants’ spin doublet $M_S = \pm 1/2$ to evolve into the component of the products’ spin doublet $M_S = \mp 1/2$ (Figures 1 and 2). If the levels of the reactants and products fulfill the diabatic condition $E_i = E_f$ when $B = 0$, a progressive increase of the magnetic induction will weaken the strength of the coupling and decrease the rate of evolution from $M_S = \pm 1/2$ (reactants) into $M_S = \mp 1/2$ (products) (Figure 1). If levels of the reactants and products differ in energy when $B = 0$, a progressive increase of B may induce crossings at B_{cross} and break such an occasional condition when $B > B_{\text{cross}}$ (Figure 2). There must be, therefore, a range of magnetic inductions where the suppression of the hfc-induced spin–flip transitions will change the reaction rate. Since the energy gap between levels of the reactants and the products will be proportional to the difference of isotropic g values, i.e., $(1/2)\beta(g_{\text{reactants}} - g_{\text{products}})B$, the energy gap between levels undergoing the induced evolution increases with B , Figure 1, but the width of the hfc interaction, $|\langle i | \hat{\lambda}_{\text{hfc}} | f \rangle| = H_{i,f}$, remains constant. Time-dependent perturbation theory shows that the increasing level separation makes the hfc-induced mixing vanish as the energy gap exceeds the width $H_{i,f}$. Since Ru(III) isotropic hfc constants are about $5 \times 10^{-3} \text{ cm}^{-1}$ and $\Delta g = (g_{\text{reactants}} - g_{\text{products}}) \approx 0.08$ for reactions among the Fe(II)/Ru(III) couples in eqs 15 and 16,²¹ the splitting of the levels will be comparable to the strength of the hfc

(20) There are several mechanisms that will provide the necessary density at the nucleus and give the perturbation some width. They are, however, intrinsically weak, and their presence in the electronic matrix element will be blurred by the more intense contributions from other perturbations.

Table 1. Application of the Cartesian Components of \hat{L} to d Orbitals

φ	$\hat{L}_z\varphi$	$(\hat{L}_x \pm i\hat{L}_y)\varphi$
z^2	0	$\mp(x^2 - y^2) - ixy \pm \sqrt{3}z^2$
xz	iyz	$i(x^2 - y^2) \mp xy + i\sqrt{3}z^2$
yz	$-ixz$	$\pm yz + ixz$
xy	$-2i(x^2 - y^2)$	$\pm\sqrt{3}xz - i\sqrt{3}yz$
$x^2 - y^2$	$2ixy$	$\pm xz - iyz$

between $B = 1.5 \times 10^{-2}$ and 5×10^{-2} T. This is the range of the magnetic induction where the effectiveness of the hfc-induced spin evolution is rendered half ineffective with associated decreases of the reaction rate. The closeness of $B_{1/2}$ in Figure 3 to the calculated range of magnetic inductions suggests that the suppression of the hfc-induced spin evolution plays a very important role in making these reactions diabatic under a zero or nearly zero, (e.g., earth intense) magnetic induction. In eq 16, the width $H_{i,f}$ must be about an order of magnitude larger to yield values of $B_{1/2}$ between 3×10^{-1} and 5×10^{-1} T. Spin-orbit-coupling-induced spin-flip transitions must therefore account for such larger values of $B_{1/2}$.

2. Spin-Orbit Coupling. The contribution of the spin-orbit coupling, SOC, to the MKE was already analyzed in relation to electron-transfer reactions of singlet coordination complexes, eq 2.^{3b} An application to electron transfer between couples of spin-paired d^5 and d^6 transition metal compounds is presented in section b of Appendix. On the basis of the time-dependent perturbation theory, one component in the $\hat{\mathcal{H}}_{SOC}$ expansion will couple off-diagonal states of the spin. Reactant states with spin projection $M_S = \mp 1/2$ will evolve into $\pm 1/2$ product states in our example of a d^6 to d^5 electron-transfer reaction. A companion change of the orbital momentum must simultaneously take place to make such time evolutions effective. Namely, an effect similar to the flip of the nuclear spin in the hfc-induced transitions considered above and in the radical pair mechanisms. The departure from the $|E_i - E_f| \leq H_{i,f}$ condition between reactant and product states under the effect of a magnetic induction has been discussed above in relation to the hfc-induced spin-flip transitions. Although the inequality is also applicable to the SOC-induced spin-flip (Figures 1 and 2), the strengths of the off-diagonal hfc and SOC matrix elements are different. Since a larger matrix element can be expected for some SOC perturbation than for the hfc, SOC-induced transitions can be effective over larger magnetic inductions than those induced by the hfc. This may not be, however, a general rule because it could be reversed, e.g., when the electronic configurations have a negligible SOC. The result of the operation with L_{\pm} on d orbitals, Table 1, shows that in a cubic symmetry, a t_{2g}^6 configuration of the reactant will be able to evolve into excited states of the product, i.e., with a $t_{2g}^5 e_g$ configuration.^{23,24} The reverse is also valid; excited states of the donor $A^{(n-1)+}$, i.e., ${}^3T_{1g}$ and/or ${}^3T_{2g}$ of a $t_{2g}^5 e_g$ configuration, will be able to evolve into the product $B^{(m-1)+}$ ground state ${}^1A_{1g}$ of a t_{2g}^6 configuration.

Although this rationalization only provides symmetry-based selection rules, it can be complemented by a constraint, $|E_i - E_f| \leq H_{i,f}$, which establishes that the energy gap between departure and arrival states be within the width of the coupling perturbation.⁹ While the ${}^3T_{1g}$ and/or ${}^3T_{2g}$ excited states of the Fe(II) reactant in eq 16 could be sufficiently close to and be effectively mixed into the ${}^1A_{1g}$ ground state at nuclear configurations close to the reaction's transition state, such a condition will be doubtfully fulfilled in eq 15 and will not be satisfied by the Ru(II) reactant in eq 17.^{24,25} When ${}^3T_{1g}$ and/or ${}^3T_{2g}$ excited states are mixed into the ground state to a considerable degree, the SOC perturbation will make possible $M_s = \pm 1/2$ states in the encounter complex to evolve into $\mp 1/2$ states of the successor complex. A rapid decrease of $k(B)/k(0)$ with $B < 0.1$ T in Figure 4 must therefore reflect the simultaneous effect of the magnetic-field-induced suppression of the SOC and hfc-promoted spin-flip transitions. Only the hfc-promoted spin evolutions, i.e., from ground to excited-state levels, will be disrupted by B when triplet excited states are not mixed with the ${}^1A_{1g}$ ground state. No participation of triplet excited states is expected in eq 17. Differences among the functional dependences of $k(B)/k(0)$ on B shown in Figures 3 and 4 on one side and Figure 5 on the other may also reflect a large contribution of the Zeeman mechanism to the spin evolution in eq 17.

3. Zeeman Mechanism. On the same basis discussed above for the hfc and SOC perturbations, the Hamiltonian's term $\hat{\mathcal{H}}_Z$ can be expanded, section c of Appendix, in terms that represent specific perturbations of the spin states. It must be noted that the Zeeman mechanism arises from three terms where the spin operators for the transferred electron and each core are grouped by pairs. This type of pairing can be seen in eq 27 of section c of Appendix. The z component of the spin, M_s , must be conserved in at least one term in order to have an active Zeeman mechanism. Also the differences between g values must not vanish in any of the terms where M_s is conserved. If a spin state of the d^5 ion A^{n+} has a spin projection $M_s = 1/2$, the mechanism will accelerate the conversion to states where the transferred electrons appear with spin projection $M_s = -1/2$. Since the z projection of the d^5 ion A^{n+} has $M_s = 1/2$ and the transferred electron has $M_s = -1/2$, the mechanism will be effective if the (electron acceptor) d^5 ion B^{m+} has a $1/2$ spin projection. Therefore, the mechanism will make electronic states of the encounter pair $[A^{(n-1)+}, B^{m+}]$ with spin projections $M_s = \pm 1/2$ evolve into states of the successor pair $[A^{n+}, B^{(m-1)+}]$ with spin projection $M_s = \pm 1/2$ with a rate proportional to B_z^2 . It must be noted that M_s is conserved in these spin evolutions.²⁵

In a previous treatment of the MKE, the wave function of each transferred electron was considered a pure spinor.^{3b} In accordance with the preceding treatment of the SOC, this approximation assumes that the transferred electrons have a negligible orbital momentum and that they behave magnetically as a free electron with $g_i \approx 2.0003 = g_{free}$. Since the value of g_i is very different from the species in eqs 15–17, the rate constants of these reactions should all be affected by a strong Zeeman mechanism that accelerates the evolution of $M_s = \pm 1/2$ reactants' states into $M_s = \pm 1/2$ products' states until saturation. This mechanism appears to be particularly important for the electron transfer between Ru compounds, eq 17 and Figure 5, since a sharp decrease of the rate constant is not observed with inductions $B < 0.1$ T. It can be argued that in eq 17, by contrast to eqs 15 and 16, the transformation of the $[A^{(n-1)+}, B^{m+}]$ spin

- (21) (a) Goodman, B. A.; Raynor, J. B. *Inorg. Radiochem.* **1970**, *13*, 135. (b) Altshuler, S. A.; Kozlyev, B. M. *Electron Paramagnetic Resonance in Compounds of Transition Metal Elements*, 2nd ed.; Wiley: New York, 1974.
- (22) (a) Reference 13a, pp 31–37. (b) Messiah, A. *Quantum Mechanics*; North-Holland: Amsterdam, 1961.
- (23) The accessibility of these excited states and their role in the Fe(II) photoinduced spin crossover has been extensively reviewed in a literature report.¹⁹ Support of the possible participation of such excited states in electron-transfer reactions is provided by this type of spin crossover and related phenomena.
- (24) Gülich, P.; Hauser, A.; Spiering, H. *Angew. Chem., Int. Ed. Engl.* **1994**, *33*, 2024.

- (25) It must be noted that under particular experimental conditions and for a certain range of B only the MKE exhibits a dependence on B characteristic of a given hfc, SOC, or Zeeman mechanism.

states into those of the pair $[A^{n+}, B^{(m-1)+}]$ is very symmetric and the magnetic induction can only change the gap between levels of the reactants and products shown in Figure 1 by a very small amount. If such a gap experiences a minor change for $B < 8$ T, hfc- and SOC-induced state evolutions will not be disrupted by the magnetic induction. Therefore, the MKE cannot reverse their contributions to $k(B)$. The only manifestation of the magnetic induction sensed through the reaction rate will come from the acceleration caused by the Zeeman mechanism. By contrast to eq 17, spin-flip and spin-rephasing transitions will be sensed in eqs 15 and 16. A reason for the dependence of $k(B)$ on B for magnetic inductions between 10^{-2} and 1 T in Figures 3 and 4 can then be related to the large difference between the $g_{av,i}$ and Δg_i values of the cores Fe(III), $g_{av} \approx 2.0$, and Ru(III), $g_{av} > 2.5$ and $\Delta g > 1.5$. A progressive increase of the rate constant with B will be kept until the magnetic induction B is greater than 1 T, where the anisotropic contributions to the Hamiltonian make the relaxation mechanism a dominant one.

Anisotropic Terms. The tapering of the MKE for magnetic inductions $B > 1$ T in Figures 3–5 can be related to the relaxation mechanism on the basis of the anisotropic components of the \mathbf{g} and \mathbf{A} tensors.^{3b} The basis of a relaxation mechanism is an external, time-dependent perturbation $V(t)$ with an auto-correlation time τ . Such a perturbation can be associated with a time-dependent anisotropic component of the Hamiltonian, $\hat{\lambda}(t) = \hat{\lambda}_{anis} V(t)$, which induces relaxations from departure states into arrival states.^{3b,26} For example, the solvent-controlled adiabatic rate is a manifestation of the dielectric relaxation in the expression of the rate constant for an outer-sphere electron transfer, eq 5. Only the isotropic components of the \mathbf{g} and \mathbf{A} tensors were considered in the preceding treatment of the isotropic terms. Their anisotropic components can be introduced in $\hat{\lambda}_{anis,HFC}$ and $\hat{\lambda}_{anis,Z}$ for the Zeeman and hfc contributions to the relaxation mechanism. The associated time-dependent perturbation $V(t)$ has been previously related to the intraligand, high-frequency vibrations and metal–ligand, low-frequency vibrations of one reactant relative to the coordinate axes of the other reactant.^{3b} One condition that largely determines the effectiveness of the mechanism is the frequency of these two types of vibrational modes. It is possible to quench the MKE and return the rate constant to its value at $B = 0$ T when the relaxation mechanism becomes very effective at large magnetic inductions. Mathematical simulations in accordance with experimental data, Figures 3–5, show that for some reactions the relaxation only causes a partial quenching of the MKE. The extent of the anisotropies in the \mathbf{g} and \mathbf{A} tensors must also be considered; i.e., the more isotropic they are, the less effective the relaxation mechanism will be.

Conclusions

This work has demonstrated a magnetic field response of electron-transfer reactions that is unequivocally nonadiabatic. The behavior observed can only be accounted for by the properties of the electronic wave function of the reaction system. Magnetic fields can therefore be used as a way to induce variations of the electronic matrix element without alterations of other parameters that determine the value of the rate constant. Methods based on the determination of magnetic-field-induced optical changes in addition to MFE in reaction rates of inner-

sphere and intervalence electron transfers may yield similar experimental information about the adiabatic character of these processes.

Acknowledgment. The work described herein was supported by the Office of Basic Energy Sciences of the U.S. Department of Energy. This is Contribution NDRL-4167 from the Notre Dame Radiation Laboratory. The author also acknowledges valuable comments by Prof. J. F. Endicott and Prof. U. Steiner about this work.

Appendix

In a literature treatment,^{3b} MKE on outer-sphere electron-transfer reactions have been rationalized on the basis of a model that is based on the quantum mechanical perturbation theory. It considers that a competition between a diabatic, k_{et}^{NAD} , electron transfer and an adiabatic dielectric relaxation, k_{et}^{AD} , contribute to the overall rate constant:

$$k_{et}^{-1} = [k_{et}^{AD}]^{-1} + [k_{et}^{NAD}]^{-1} \quad (4)$$

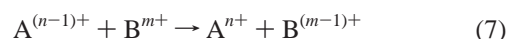
Equation 4 is a variation of the previously discussed expression for k_{et} , eq 1, and has the NAD and AD contributions defined on the basis of the first-order potential surfaces.^{10a,c} A literature expression for k_{et}^{NAD} , eq 5, depends on the “Marcus activation energy”, E_a , the solvent reorganization energy, E_r , and the square of the electronic matrix element $|\langle i | \hat{\lambda}_{xchg} | f \rangle|^2$.⁹

$$k_{et}^{NAD} = \frac{2\pi |\langle i | \hat{\lambda}_{xchg} | f \rangle|^2}{\hbar(4\pi E_r k_B T)} \exp\left(-\frac{E_a}{k_B T}\right) \quad (5)$$

The adiabatic contribution, k_{et}^{AD} , is inversely proportional to the lifetime for the longitudinal solvent relaxation, τ_L .¹⁰

$$k_{et}^{AD} = \tau_L^{-1} \frac{E_r}{16\pi k_B T} \exp\left(-\frac{(\Delta E - E_r)^2}{4E_r k_B T}\right) \quad (6)$$

In the absence of a magnetic induction, an expansion of the Hamiltonian, $\hat{\lambda}_{xchg}$, has been previously given for the diabatic transfer of one electron, eq 5, between a pair of ions:¹²



It must be noted that the two basis sets $\langle i |$ and $\langle f |$, correspond to the localization of the electron in either center, $A^{(n-1)+}$ or $B^{(m-1)+}$, and they are not orthogonal. A suggested approach to the time-dependent perturbation theory uses the wave functions for the “cores”, i.e., the species missing the exchanged electron.^{9a} In eq 7 the cores are, therefore, the oxidant B^{m+} and the oxidized reductant, A^{n+} . It is possible to express the wave function of the state $\langle i |$, eq 8, by using Slater wave functions $A^{(n-1)+}$ and B^{m+} and the nuclear spin wave functions $\langle u_A |$ and $\langle u_B |$.

$$\langle i | = |A^{(n-1)+} \rangle |B^{m+} \rangle \langle u_A | \cdot \langle u_B | \quad (8)$$

If one applies the *Laplace development* to the Slater determinant $A^{(n-1)+}$, eq 8 can be recast into eq 9, where A_t^{n+} is the cofactor of $\langle t |$.¹³

$$\langle i | = \left(\sum_t |A_t^{n+} \rangle \langle t | \right) |B^{m+} \rangle + \langle u_A | \cdot \langle u_B | \quad (9)$$

It must be noted that the expansion of $A^{(n-1)+}$ in eq 9 is made along a row that includes all the equivalent and transferrable electrons t of the donor with spin–orbital wave functions $\langle t |$.

(26) (a) Carrington, A.; McLachlan, A. D. *Introduction to Magnetic Resonance*; Harper & Row: New York, 1967; Chapter 11. (b) Redfield, A. G. *IBM J. Res. Dev.* **1957**, 19.

The cofactors $|A_t^{n+}|$ represent, therefore, various electronic configurations of the *core* A^{n+} . A similar expansion, eq 10, can be applied to the final state $\langle f|$.

$$\langle f| = \left(\sum_t |A_t^{n+}| \right) \left(\sum_{t'} |B_{t'}^{m+}| \langle t' | \right) \langle \mu_A | \langle \mu_B | \quad (10)$$

While antisymmetrized multielectron wave functions may be required for the correct treatment of a Hamiltonian containing two-electron terms, the wave functions in eqs 9 and 10 suffice for the qualitative treatment of the one-electron magnetic perturbations. The literature Hamiltonian \hat{H}_{chng} included numerous interactions of the exchanged electron but did not consider the spin phenomena that account for the dependence of the specific rate of outer-sphere electron-transfer reactions on the magnetic induction B .¹² An addition made to the Hamiltonian in eq 5 incorporated the couplings of the electronic spin to the nuclear spin, \hat{H}_{hfc} , and to the orbital angular momenta, \hat{H}_{SOC} , of the chemical system.^{3b} It also included Zeeman interactions, \hat{H}_{Z} , dictated by the coupling of the electronic spin to a magnetic induction. Explicit forms of \hat{H}_{SOC} , \hat{H}_{hfc} , and \hat{H}_{Z} for spin-paired d^5 and d^6 ions in eq 7 will be given below.

The isotropic components of \hat{H}_{hfc} and \hat{H}_{SOC} allow reactant states to evolve with a finite rate into some product states that in a zero-order approximation have $|\langle i | \hat{H}_{\text{chng}} | f \rangle|^2 = 0$ (Figures 1 and 2). Since the SOC and hfc induce conversions, spin-flip transitions, between states when they obey the relationship $|E_i - E_f| \leq H_{\text{rf}}$, the energy gap created by a magnetic induction makes the rate of evolution dependent on B . The B -dependent Zeeman perturbation, $\hat{H}_{\text{Z}} \propto B$, accelerates the evolution among states with the same spin projection, e.g., the T_0 -S rephasing transitions in encounter pairs of doublet radicals.

Time-dependent perturbations related to anisotropic terms in the Hamiltonian, $\hat{H}_{\text{hfc,an}}$ and $\hat{H}_{\text{Z,an}}$, induce the evolution from spin levels of the reactants to the products.¹⁵ The mechanism bears some resemblance to the rotationally induced spin relaxation in radical pairs.¹⁶

a. The contact interaction operator is given in

$$\hat{H}_{\text{hfc}} = \sum_t \frac{1}{n_t} [\mathcal{P}_{t,A} (\hat{S}_{A,t} \sum_i A_{i,A,t} \hat{I}_{i,A,t} + \hat{S}_{t,A,t} \hat{I}_{t,A,t})] + \hat{S}_B \sum_k A_{k,B} \hat{I}_{k,B} \quad (18)$$

The summation in the first term includes all the n_t equivalent electrons, t , that can be transferred from $A^{(n-1)+}$. Nuclear and electronic spin operator of a given species, A^{n+} , B^{m+} , are respectively represented by $\hat{S}_{A,t}$, $\hat{I}_{t,A}$, \hat{S}_B , $\hat{I}_{k,B}$ and those for a transferred electron, t , by \hat{S}_t , $\hat{I}_{t,A}$. An operator $\mathcal{P}_{t,A}$ permutes a given transferable electron, t , with another transferable electron in the *core* A^{n+} . Since the contact interaction demands electronic wave functions with density at the nucleus, $A_{t,A}$ will be very small and the contact interaction of the transferred electron can be neglected:²⁰

$$\begin{aligned} \hat{H}_{\text{hfc}} &= \sum_t \frac{1}{n_t} [\mathcal{P}_{t,A} (\hat{S}_{A,t} \sum_i A_{i,A,t} \hat{I}_{i,A,t})] + \hat{S}_B \sum_k A_{k,B} \hat{I}_{k,B} \\ &= \frac{1}{n_t} \sum_t \mathcal{P}_{t,A} [\hat{H}_{\text{hfc}}^+(B,A,t) + \hat{H}_{\text{hfc}}^-(B,A,t)] \quad (19) \end{aligned}$$

The expression following the second equal sign in eq 19 was derived by using one of various manners, to group the individual

$$\begin{aligned} \hat{H}_{\text{hfc}}^+(B,A,t) &= ({}^{1/2}) (\hat{S}_{A,t} + \hat{S}_B) \left(\sum_i A_{i,A,t} \hat{I}_{i,A,t} + \sum_k A_{k,B} \hat{I}_{k,B} \right) \\ \hat{H}_{\text{hfc}}^-(B,A,t) &= ({}^{1/2}) (\hat{S}_{A,t} - \hat{S}_B) \left(\sum_i A_{i,A,t} \hat{I}_{i,A,t} - \sum_k A_{k,B} \hat{I}_{k,B} \right) \quad (20) \end{aligned}$$

operators by means of rising and lowering operators. In this grouping, the $\hat{H}_{\text{hfc}}^{\pm}(B,A,t)$ operator is diagonal in the nuclear-electronic spin basis of the *cores* and only induces a shift in their energies. The expression for $[\hat{H}_{\text{hfc}}^{\pm}(B,A,t)]$ is given in

$$\begin{aligned} \hat{H}_{\text{hfc}}^{\pm}(B,A,t) &= (\hat{S}_{A,t}^z - \hat{S}_B^z) \left(\sum_i A_{i,A,t} \hat{I}_{i,A,t}^z - \sum_k A_{k,B} \hat{I}_{k,B}^z \right) + \\ &({}^{1/2}) (\hat{S}_{A,t} - \hat{S}_B) \left(\sum_i A_{i,A,t} \hat{I}_{i,A,t} - \sum_k A_{k,B} \hat{I}_{k,B} \right) + \\ &({}^{1/2}) (\hat{S}_{A,t} + \hat{S}_B) \left(\sum_i A_{i,A,t} \hat{I}_{i,A,t}^+ - \sum_k A_{k,B} \hat{I}_{k,B}^+ \right) \quad (21) \end{aligned}$$

Superscripts z in eq 21 denote the corresponding coordinate projection of an operator and superscripts $+$ and $-$ indicate a rising, $+$, or lowering, $-$, operator. The second and third terms allow spin-forbidden evolutions from the initial to the final states in finite times if a change of the electronic spin is counterbalanced by a change in nuclear spin.

b. A more general treatment of the SOC is given next for electron transfers from a low-spin d^6 to a low-spin d^5 transition metal compound, eq 11. The SOC treatment has to be based on

$$\hat{H}_{\text{SOC}} = \sum_{\mu=1}^N \sum_{j=1}^n \xi(r_{\mu,j}) \hat{I}_{\mu,j} \hat{S}_j \quad (22)$$

where

$$\xi(r_{\mu,j}) = \frac{1}{2m^2 c^2} \left(\frac{1}{r_{\mu,j}} \frac{d}{dr_{\mu,j}} V_{\mu,j} \right)$$

a primary result of relativistic quantum mechanics rather than those commonly used with intramolecular phenomenon.^{13,22}

The summations run over all the nuclei, $N \geq \mu \geq 1$, and over all the electrons, $n \geq j \geq 1$, with each electron j moving under the spherically symmetric potential, $V_{\mu,j}$, of the μ nucleus. Equation 22 can be condensed into a more manageable one by grouping in terms of the *cores* and a transferable electron. This approximation is based on the assumption that the transferred electron will be subjected to a Coulombic potential much different from the other electrons. To satisfy the uncertainty principle, all equivalent transferable electrons should be subjected to such a condition and represented in \hat{H}_{SOC} with a $1/n_t$ weight, where n_t is the total number of equivalent transferable electrons from the donor $A^{(n-1)+}$. In terms of the *cores* A^{n+} and B^{m+} and the various transferable electrons, eq 22 is reduced to eq 23.

$$\begin{aligned} \hat{H}_{\text{SOC}} &= \sum_{\mu=1}^{N_A} \left[\sum_t \frac{1}{n_t} \mathcal{P}_{t,A} (\xi(r_{\mu,t}) \hat{I}_{\mu,t} \hat{S}_t + \sum_{j=1}^{n_A-1} \xi(r_{\mu,j}) \hat{I}_{\mu,j} \hat{S}_j) \right] + \\ &\sum_{\mu=1}^{N_A} \sum_{j=1}^{n_B} \xi(r_{\mu,j}) \hat{I}_{\mu,j} \hat{S}_j + \sum_{\mu=1}^{N_B} \sum_{j=1}^{n_B} \xi(r_{\mu,j}) \hat{I}_{\mu,j} \hat{S}_j + \sum_{\mu=1}^{N_B} \sum_{j=1}^{n_A} \xi(r_{\mu,j}) \hat{I}_{\mu,j} \hat{S}_j \quad (23) \end{aligned}$$

The summations of electrons 1 to n_B over N_B nuclei in B^{m+} and 1 to n_A over N_A nuclei in A^{n+} are the intramolecular SOC

of these species, while the cross summations represent the interaction of a given electron with its orbital momentum in other nuclei.²² The operator $\mathcal{P}_{t,A}$ provides permutations between transferable electrons, t , and other transferable electrons in A^{n+} in the same manner as the hfc problem. Equation 23 can be recast in a more condensed form by grouping the various summations:

$$\hat{H}_{\text{SOC}} = \left[\sum_t \frac{1}{n_t} \mathcal{P}_{t,A} (\lambda_{A,t} \hat{L}_{A,t} \hat{S}_A + \xi(r_{A,t}) \hat{I}_{A,t} \hat{s}_t) \right] + \lambda_{AB} \hat{L}_A \hat{S}_B + \lambda_B \hat{L}_B \hat{S}_B + \lambda_{BA} \hat{L}_B \hat{S}_A \quad (24)$$

A further simplification,

$$\hat{H}_{\text{SOC}} = \frac{1}{n_t} \sum_t [\lambda_B \hat{L}_B \hat{S}_B + \mathcal{P}_{t,A} (\lambda_{A,t} \hat{L}_{A,t} \hat{S}_A)] + \lambda_{AB} \hat{L}_A \hat{S}_B + \lambda_{BA} \hat{L}_B \hat{S}_A \quad (25)$$

results when the orbital momentum of the transferred electron is regarded as negligible on the presumption that its motion will resemble more a radial displacement than an angular one.

Similarities with the hfc perturbation, eq 21, become evident when the very small cross interactions in the second and third terms of \hat{H}_{SOC} are ignored and shift operators L_{\pm} and S_{\pm} are used for the expansion of the contents of the bracket in eq 25.

c. It is possible to express the Hamiltonian for the Zeeman perturbation, \hat{H}_Z , in terms of the three contributions shown in eq 26.^{3b}

$$\hat{H}_Z = \sum_t \frac{1}{n_t} [\mathcal{P}_{t,A} (g_B \beta B_z \hat{s}_{z,t} + g_{A,t} \beta B_z \hat{S}_{z,A,t})] + g_B \beta B_z \hat{S}_{z,B} \quad (26)$$

The summation over the (equivalent) transferable electrons t includes two terms, the Zeeman perturbation over the transferred

electron and the associated electronic configuration in the core A^{n+} . The third term represents the perturbation of the z component of the magnetic induction, B_z , on the spin states of the core B^{m+} . Other symbols in eq 26 were already defined in parts a and b of Appendix. The expansion of eq 26 by means of literature-defined shift operators leads to eq 27.^{3b}

$$\begin{aligned} \hat{H}_Z = & \sum_t \frac{1}{n_t} [\mathcal{P}_{t,A} \{ (g_B + g_t + g_{A,t}) \beta B_z (\hat{S}_{z,B} + \hat{s}_{z,t} + \hat{S}_{z,A,t}) \}] + \\ & ({}^{1/3}) \sum_t \frac{1}{n_t} [\mathcal{P}_{t,A} \{ (g_{A,t} - g_B) \beta B_z \mathcal{P}_{t,A} (\hat{S}_{z,A,t} - \hat{S}_{z,B}) \}] + \\ & ({}^{1/3}) \sum_t \frac{1}{n_t} [\mathcal{P}_{t,A} \{ (g_{A,t} - g_t) \beta B_z \mathcal{P}_{t,A} (\hat{S}_{z,A,t} - \hat{s}_{z,t}) \}] + \\ & ({}^{1/3}) \sum_t \frac{1}{n_t} [\mathcal{P}_{t,A} \{ (g_B - g_t) \beta B_z (\hat{S}_{z,B} - \hat{s}_{z,t}) \}] \quad (27) \end{aligned}$$

The first term in eq 27 only causes an isotropic shift in the energy of electronic levels while the three following terms induce the evolution of the spin with a strength directly proportional to the square of the applied magnetic induction, B_z^2 . The time-dependent evolution of a reactant state into a product state is therefore controlled by the last three terms, and the first one can be ignored. In contrast to the hfc and SOC contributions, the magnetic induction in the Zeeman mechanism accelerates the conversion between such states and the magnetic field acceleration is continued until the mechanism reaches saturation. Factors expressing a difference between the g values of various species also determine the weight of the terms associated with the Zeeman mechanism. If the cores A^{n+} and B^{m+} have nearly identical g values, they will occasionally approach the value of g_t and make all three terms insignificantly small.

IC991174O